




Seismic Responses of Near-Fault Building-Structure Groups in the Vicinity of the Basin Edge

Wei Zhong^{1, 2} 

¹Xichang University, Xichang, P. R. China

²Chongqing College of Electronic Engineering, Chongqing, P. R. China

jnewore@163.com

Abstract. Earthquakes often lead to severe earthquake disasters in cities near fault zones, especially in cities on the surface of basins. To study the basin edge effects on seismic responses of near-fault building-structure groups, an integrated numerical method is adopted and two identical structure clusters inside and outside the basin edge are considered. The seismic responses of two near-fault building-structure groups in the vicinity of basin edge are modelled during an earthquake of M_w 6.0. Comparing to the structures outside the basin edge, the bending moments of plane frame structures inside the basin edge are increased significantly, and the basin edge effect changes earthquake risk positions of the structures. The vertical displacements of the structures are increased and the horizontal displacements of the structures are decreased slightly. The detailed geological structure of basin needs to be considered when modelling seismic responses of near-fault structure groups.

Keywords: Basin edge; Seismic responses; Building-structure groups; Near-fault; Investigated lump

1 INSTRUCTION

It was shown that the existence of basin affects greatly on ground motions, and then the detailed basin's subsurface geology needs to be known in simulating ground motions [1, 2]. The concerned basins include San Fernando basin, San Bernardino basin and the Los Angeles basin. The urban structures at the surface of the basins are usually overlooked and the earthquake responses of structures cannot be obtained. Actually, there exist a number of urban structure clusters in the basin region. Furthermore, the seismic responses of the structures are an important factor causing severe seismic hazard in urban area. So, a rational computational model not only should include earth media and seismic sources but also include urban building-structure groups.

A few researchers combined the urban structure clusters on the basin with earth media and finite-fault seismic sources to research site-city interaction (SCI) near fault during an earthquake. Introducing the urban building-structure groups, Guidotti et al. [3] studied the issue of SCI during 2011 Christchurch earthquake of M_w 6.2. The studied area is Christchurch Central Business District including around 150 buildings, which is

© The Author(s) 2024

B. Yuan et al. (eds.), *Proceedings of the 2024 8th International Conference on Civil Architecture and Structural Engineering (ICCASE 2024)*, Atlantis Highlights in Engineering 33,

https://doi.org/10.2991/978-94-6463-449-5_74

located inside the alluvial basin. It was shown that the existence of the urban building-structure groups affects significantly ground-motion characteristics inside Christchurch city. Isbiliroglu et al. [4] studied SCI effects on seismic responses of building-structure groups during an earthquake. In the works mentioned above, a type of simplified low-velocity block was used for representing a building or a set of buildings in city. This simplified building model was first introduced into studying site-city interaction [5]. However, this type of simplified building model neglected the internal details of real building structure, and then cannot be used for obtaining the actual internal forces and deformations, that are the actual seismic responses focused on in civil engineering, of structural members.

Thus, it is necessary to introduce the building-structure model which can obtain the actual seismic structural responses. In our previous work [6], introducing a member model for plane frame structure, an integrated system, which is constituted by frame structure groups, viscoelastic half-space and fault, was constructed. Using this integrated system, an integrated method has been developed for simulating structural flexural wave propagation, earth-medium viscoelastic wave propagation and bidirectional wave propagation between the soil medium and near-fault structures during an earthquake.

To understand basin-edge effects on earthquake responses of structure groups near fault, using an integrated method [6] and considering two identical building-structure groups, which are respectively situated on the sites inside and outside the basin edge, the author will model seismic responses of frame structure groups during a hypothetical earthquake of M_w 6.0. And then the author will study the basin edge effects on bending moments of structures in groups, earthquake risk positions of all structures and snapshots of displacement of all structures.

2 THE INTEGRATED METHOD FOR MODELLING WAVE PROPAGATION IN THE INTEGRATED SYSTEM

In this article, as is shown in Figure 1(a), the integrated system is composed of plane frame structure groups, viscoelastic half-space and fault. To implement integrated numerical method for modelling seismic wave propagation in the system, three kinds of the investigated lumps have been constructed [6-8]: ① the structural investigated lump, ② the earth-medium investigated lump and ③ the connecting investigated lump. As is shown in Figures 1(b) and (c), these three kinds of investigated lumps in the system are respectively represented by shaded parts A1, A2 and A3.

In our previous work [6], the governing equations for these three kinds of investigated lumps have been established, and then the integrated numerical method has been implemented by time-domain iteration. In summarize, there are four steps to implement the method: Step 1. Calculate the accelerations of three types of investigated lumps at time t_0 from the interior forces acting on the contour (for A2, A3) and/or median cross-section (for A1, A3) by dynamic equilibrium equations. Step 2. Calculate the displacements of three types of investigated lumps at time $t_0 + \Delta t$ by doing twice time integrations. Step 3. Calculate the interior forces acting on the contour (for A2, A3) and/or

median cross-section (for A1, A3) at time $t_0+\Delta t$ by viscoelastic constitutive equations (for A2, A3) and/or calculating formula of median cross-section internal forces (for A1, A3). Step 4. Calculate the accelerations of three types of investigated lumps at time $t_0+\Delta t$ as they have been done in step 1.

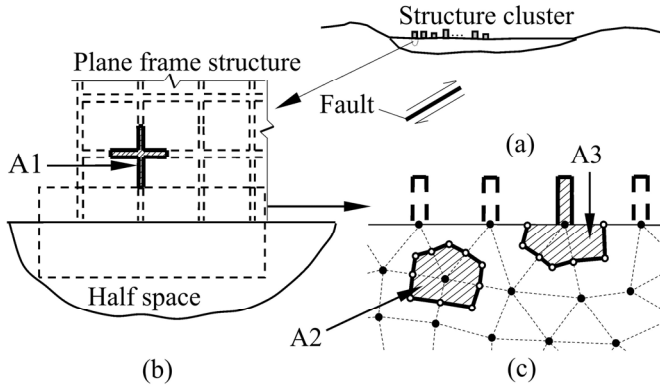


Fig. 1. The integrated system (a) and the three investigated lumps (shaded parts A1, A2, A3 shown in (b) and (c)).

It is simple to implement the program of this method. Firstly, the structure model and half-space model only need to be built independently. Secondly, the computer only needs to know which investigated lump in bottom columns of structures and which investigated lump of the earth's surface belong to the same connecting investigated lump.

3 NUMERICAL SIMULATION

3.1 Computational Model

As is depicted in Figure 2, the computational model is composed of three components: frame structure groups, earth media and seismic source.

For the frame structure groups, the author considers two identical building-structure groups S1 and S2, which are respectively situated inside and outside the basin. The epicentral distances of the two groups' centers are respectively 6.08 km and 7.74 km. Each group consists of 10 3-bay 6-storey RC plane frame structures (the structures from left to right are represented by symbols b1-b10, respectively) with equal spacing of 27.6 m. Each span of all the structures is 6.9 m. The strength grade of concrete for all structural members is C25. The mass density and elastic modulus of concrete are respectively 2500 kg/m^3 and $2.8 \times 10^{10} \text{ N/m}^2$.

For the earth media, the geological structure consists of half-space bedrock, sedimentary layer and basin. The basin's length is 3.1 km. The basin's maximum depth under earth's surface is 450 m. The distance of the basin's center is about 5.18 km far from the epicenter. The maximum depth of sedimentary is 1.0 km. The material properties of earth media are listed in the table in the bottom-right of Figure 2.

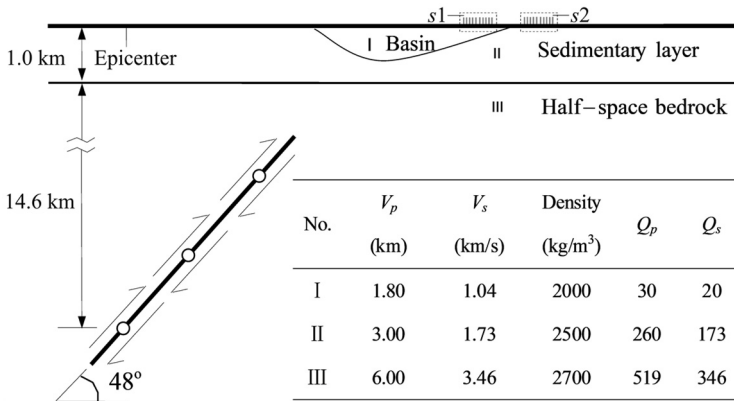


Fig. 2. The computational model and the material properties of earth media. The three circles denote three subfaults.

For the seismic source, the finite-fault source model is adopted herein [6, 9]. For a M_w 6.0 earthquake, each subfault’s size is about 2.5 km. The subfaults’ number along the dip-slip direction is 3. Each subfault’s final slip displacement is around 0.35 m. Each subfault’s average rise time is approximately 2.0 s. As is shown in Figure 2, the dip angle is set about 48° and the top edge’s depth of fault plane under the earth’s surface is about 11.0 km.

3.2 Simulation Results

Figure 3 shows time histories of the bending moments of near-fault building groups inside and outside the basin edge during a M_w 6.0 earthquake. The symbol circle denotes the peak bending moment in time domain at the output point for each structure. Each output point is the left beam-end of the first span and first story of the structures b1-b10 in groups S1 and S2. Comparing to the building structures outside the basin, the increasing rate of the peak bending moments is about 8.5% (b10) ~ 19.6% (b4) for the building structures inside the basin edge. It is shown that the bending moments of frame structures in the group S1 inside the basin edge are increased significantly. For the group S1 inside the basin edge, it can be also seen that the peak bending moments of the structures b1-b6 are significantly larger than those of the structures b7-b10. The region from b1 to b6 could be location of the damage belt due to basin-edge effect, which is formed by the coincident interference between primary S-waves and diffraction/surface waves due to basin [10].

Figure 4 shows the positions, where maximum peak shear force for all column-medians of each structure is located or where maximum peak bending moment for all beam-ends of each structure in the groups S1 and S2. These positions are also named as earthquake risk positions of frame structures.

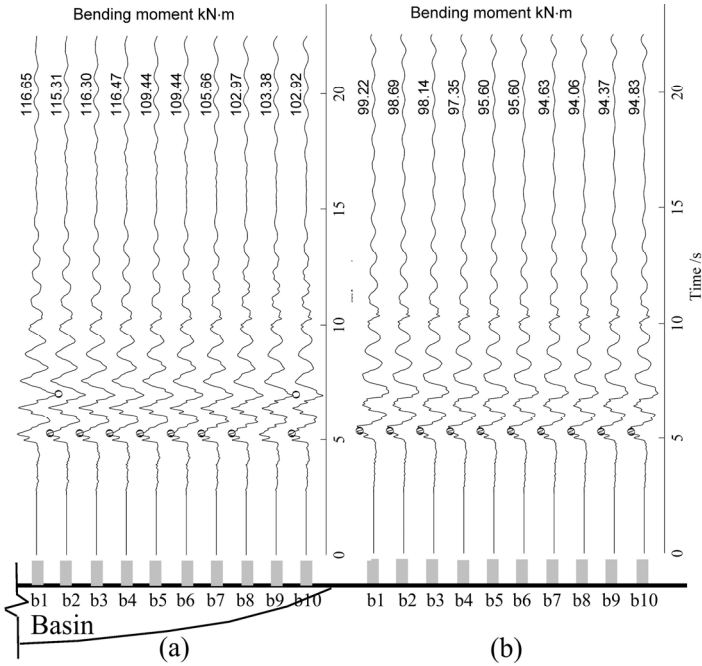


Fig. 3. The bending moments of building groups (a) inside the basin edge and (b) outside the basin edge during an earthquake of M_w 6.0.

For the structures (i.e. b1-b10 in S2) outside the basin edge as shown in Figure 4(b), the earthquake risk positions in the structures are mainly located on the first story. For the structures (i.e. b1-b10 in S1) inside the basin edge as shown in Figure 4(a), the earthquake risk positions are mainly located on the first story and the second story. The simulating results show that presence of the basin edge effect changes the earthquake risk positions of frame structures inside the basin.

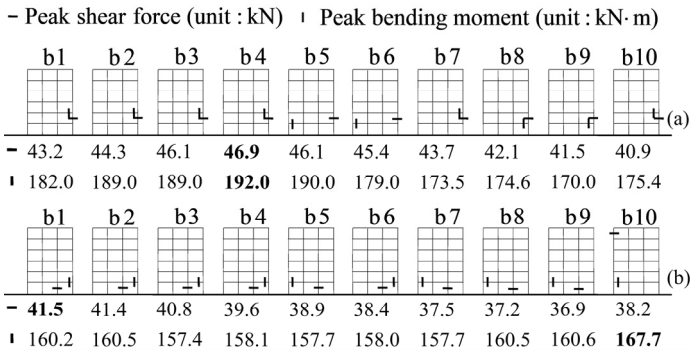


Fig. 4. Earthquake risk positions of the structures in the groups S1 (a) and S2 (b) during a M_w 6.0 hypothetical earthquake.

Figure 5 shows the displacements of all the structures in group S1 inside the basin edge and group S2 outside the basin edge at time 6.0 s after initial rupture of the fault. The displacements include displacements of ground motions and displacements caused by structural deformation. It can be seen that the vertical displacements of each structure are larger than its horizontal displacements. This may be owing to the location over the fault for the structures and small epicenter distance. Comparing to the case of the structures outside the basin edge, the horizontal displacement of each structure inside the basin edge is smaller; the vertical displacement of each structure inside the basin edge is larger. This means the basin edge effect increases the vertical displacement and decreases the horizontal displacement for the structures inside the basin edge.

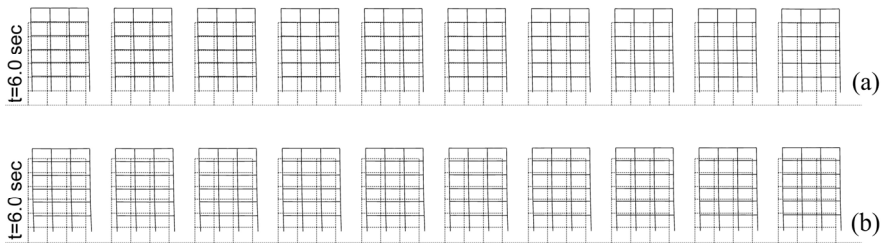


Fig. 5. Snapshots of displacements of all the structures in the clusters S1 (a) and S2 (b) at time 6.0 s after initial rupture of the causative fault. The deformations of the structures are magnified 50 times here.

4 CONCLUSIONS

An integrated method is used for obtaining seismic responses of the two identical building-structure groups in the vicinity of a basin situated on hanging wall due to rupture of thrust fault. Compared seismic responses of the building-structure group inside the basin edge with those of the group outside the basin edge, the basin-edge effects on seismic responses of the near-fault building-structure group on the basin are studied during a M_w 6.0 earthquake. The bending moments, earthquake risk positions and snapshots of displacements for all the frame structures are given in the two groups inside and outside the basin edge. Some results and conclusions are given as follows:

(1) The basin edge effect increases significantly the seismic responses of structure cluster inside the basin edge.

(2) The earthquake risk positions of frame structures inside the basin edge are different from those of frame structures outside the basin edge.

(3) The basin edge effect is prone to increase the vertical displacements and decrease the horizontal displacement for the structures inside the basin edge.

From the aforementioned results and conclusions, the detailed basin's geological structure needs to be known and should not be overlooked in studying seismic responses of near-fault building-structure groups caused by rupture of fault.

In the future work, the author will attempt to consider the nonlinear behavior of soil and structure and introduce three-dimension integrated system to obtain more actual seismic responses of building-structure groups near fault caused by rupture of fault.

The research results obtained by the integrated method can be used for explanation and prediction of seismic damage phenomenon of near-fault building-structure groups in urban area, reasonable site selection and layout of the proposed new building cluster as well as disaster relief plan for possible earthquake. It is helpful to improve the resistance of modern cities against earthquake, in order to serve for reducing earthquake disaster in urban areas.

ACKNOWLEDGMENTS

This research work is supported by Natural Science Foundation of Chongqing, China (Grant No. cstc2020jcyj-msxmX0744) and Dr's Scientific Research Start-up Project of Xichang University (Grant No. YBZ202232).

REFERENCES

1. Pitarka, A., Irikura, K. (1996) Basin structure effects on long-period strong motions in the San Fernando valley and the Los Angeles basin from the 1994 Northridge earthquake and an aftershock. *Bulletin of the Seismological Society of America*, 86: S126–S137. <https://doi.org/10.1785/BSSA08601BS126>.
2. Graves, R.W., Wald, D.J. (2004) Observed and simulated ground motions in the San Bernardino basin region for the Hector Mine, California, earthquake. *Bulletin of the Seismological Society of America*, 94: 131–146. <https://doi.org/10.1785/0120030025>.
3. Guidotti, R., Mazzieri, I., Stupazzini, M., Dagna, P. (2012) 3D numerical simulation of the site-city Interaction during the 22 February 2011 Mw 6.2 Christchurch earthquake. In: 15th World Conference of Earthquake Engineering. Portugal: Lisbon. https://www.iitk.ac.in/nicee/wcee/article/WCEE2012_2290.pdf.
4. Isbiliroglu, Y., Taborda, R., Bielak, J. (2015) Coupled soil-structure interaction effects of building clusters during earthquakes. *Earthquake Spectra*, 31: 463–500. <https://doi.org/10.1193/102412EQS315M>.
5. Wirgin, A., Bard, P.Y. (1996) Effects of buildings on the duration and amplitude of ground motion in Mexico city. *Bulletin of the Seismological Society of America*, 86: 914–920. <https://doi.org/10.1785/BSSA0860030914>.
6. Liu, T., Zhong, W. (2017) Earthquake responses of near-fault building clusters in mountain city considering viscoelasticity of earth medium and process of fault rupture. *Soil Dynamics and Earthquake Engineering*, 99: 137–141. <https://doi.org/10.1016/j.soildyn.2017.05.012>.
7. Liu, T., Zhong, W. (2014) Earthquake responses of near-fault frame structure clusters due to thrust fault by using flexural wave method and viscoelastic model of earth medium. *Soil Dynamics and Earthquake Engineering*, 61–62: 57–62. <https://doi.org/10.1016/j.soildyn.2014.01.023>.
8. Zhong, W., Liu, T. (2016) Application of an investigated lump method to the simulation of ground motion for Beichuan town during the Wenchuan earthquake. *Journal of Earthquake and Tsunami*, 10: 1650002. <https://doi.org/10.1142/S1793431116500020>.
9. Zhong, W., Liu, T. (2022) A mesh grading technique for near-fault seismic wave propagation in large velocity-contrast viscoelastic earth media. *Journal of Earthquake Engineering*, 26: 1388–1415. <https://doi.org/10.1080/13632469.2020.1719240>.

10. Kawase, H. (1996) The cause of the damage belt in Kobe: "The basin-edge effect," constructive interference of the direct S-wave with the basin-induced diffracted/Rayleigh waves. *Seismological Research Letters*, 67: 25–34. <https://doi.org/10.1785/gssrl.67.5.25>.

Open Access This chapter is licensed under the terms of the Creative Commons Attribution-NonCommercial 4.0 International License (<http://creativecommons.org/licenses/by-nc/4.0/>), which permits any noncommercial use, sharing, adaptation, distribution and reproduction in any medium or format, as long as you give appropriate credit to the original author(s) and the source, provide a link to the Creative Commons license and indicate if changes were made.

The images or other third party material in this chapter are included in the chapter's Creative Commons license, unless indicated otherwise in a credit line to the material. If material is not included in the chapter's Creative Commons license and your intended use is not permitted by statutory regulation or exceeds the permitted use, you will need to obtain permission directly from the copyright holder.

